

COMPACT FOLDED SUBSTRATE INTEGRATED WAVEGUIDE CAVITIES AND BANDPASS FILTER

R. Wang, L.-S. Wu, and X.-L. Zhou

Center for Microwave and RF Technologies
Shanghai Jiaotong University
Shanghai 200240, China

Abstract—In this paper, a folded substrate integrated waveguide (FSIW) cavity is analyzed theoretically. Formulae for the determination of the dimensions of the FSIW cavity have been deduced. To verify the proposed formulae, simulated results are compared with the results of the formulae and good agreement has been observed between them. An example filter working at 8 GHz is designed and fabricated. Good agreement between the simulated and the measured results has been obtained. Result shows the advantage of wide out-of-band rejection and compact size.

1. INTRODUCTION

With the rapid development of high quality microwave and millimeter wave communication systems, there exists a constant great demand on high-performance narrow bandpass filter with low cost, sharp selectivity, compact size, and low insertion loss. Rectangular waveguide (RW) bandpass filters have excellent performance but it is expensive and hard to fabricate whilst it has bulky volume and thus is difficult to integrate with other planar circuits. Substrate integrated waveguide (SIW) has been proposed as a new planar structure which is suitable for PCB and LTCC fabrication process [1,2]. Theoretical analysis has been carried out to investigate the propagation characteristics and discontinuities of SIW [3–5]. SIW retains main properties of rectangular waveguide (RW) like high Q and low loss. But It is easier to fabricate and integrate with other planar circuits. A great deal of applications using SIW technology has been reported [6–13].

Chen et al. [14] discussed the properties of folded rectangular waveguide whilst Grigoropoulos et al. [15] proposed the concept

and configuration of folded substrate integrated waveguide (FSIW). They concluded that FSIW retains similar cutoff and propagation characteristics while is only half the size of its equivalent SIW structure. Theoretical study of FSIW was carried out in [16]. There have already been some applications in filters and antennas to show the advantage of size reduction [17–19]. In [20], two kinds of folded-waveguide cavities were proposed and compared. The relationship between these two cavities and the conventional waveguide cavity has been found out. FSIW quarter-wavelength cavity has been used to design a bandpass filter recently [21]. Also in [22] another type of folded resonator has been proposed and employed to design a bandpass filter which exhibits good performance and compact size.

In this paper, formulae of the quarter-wavelength cavity have been derived and verified by full-wave simulation. An example filter working at 8 GHz is presented. Good agreement between simulated and measured results has been obtained. In addition, wide out-of-band rejection can be observed, which provides evidence for the analysis of the quarter-wavelength resonator.

2. THEORETICAL ANALYSIS

Figure 1 shows the configuration of a FSIW cavity, where a_{FSIW} and l_{FSIW} is the width and length of the cavity, respectively, g is the width of slot in the central plane, s is the distance between the slot and metallic via-holes, and d is the diameter of the via-holes. According to [20], when a_{FSIW} and l_{FSIW} are almost half the size of a SIW cavity, FSIW cavity resonates at approximately the same frequency as the SIW cavity. Thus, a great advantage of this structure is that it only possesses one quarter the area and one half the volume of the corresponding SIW cavity.

2.1. Eigenmodes Problem

Due to the symmetry of the structure, the fields in the upper and lower halves should be symmetric to the central plane. Even and odd modes are shown in Figure 2.

In the cases of even modes, the gap is treated as Electric Wall (EW) and thus the magnetic force lines close respectively in the upper and lower halves of the FSIW cavity. So the length of central plane equals $n/2$ guided wavelengths and thus the even modes correspond to $TE_{(2m)0(2n)}$ in the RW cavity.

In the cases of odd modes, the gap is treated as Magnetic Wall (MW) and the magnetic force lines near the gap close across the central

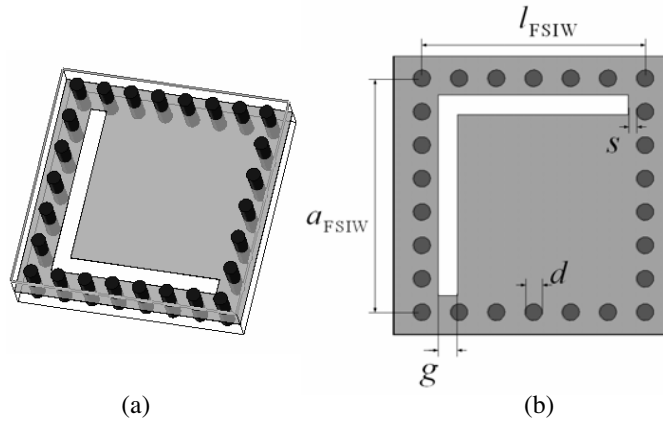


Figure 1. Configuration of the FSIW cavity. (a) 3D geometry; (b) Top view.

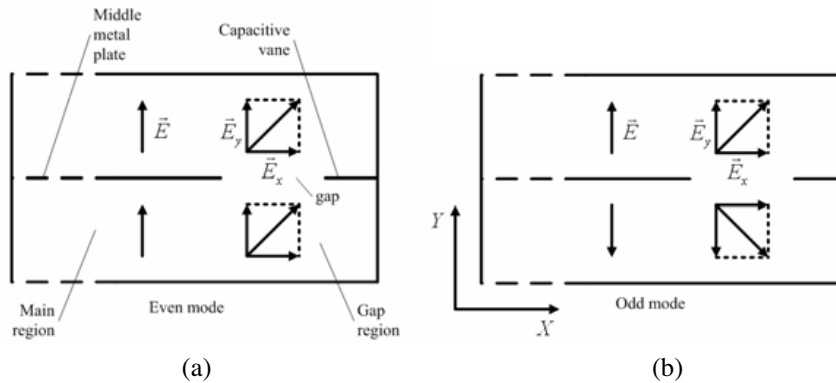


Figure 2. (a) Even and (b) odd modes in FSIW cavity.

plane. This reveals that the length of the middle metallic plate is equal to $n/2 - 1/4$ guided wavelengths. Therefore the odd modes correspond to $TE_{(2m-1)0(2n-1)}$ in RW cavity.

It can be concluded that $TE_{(2m)0(2n-1)}$ or $TE_{(2m-1)0(2n)}$ modes in the traditional RW cavity cannot exist in this folded waveguide cavity. Microwave circuits implemented with this type of cavities provide wider rejection band than traditional RW cavities. When the cavity is excited by stripline where the directions of fields are opposite in the upper and lower halves, this type of filters can only support fields similar to the odd modes in quarter-wavelength resonator. In this case, TE_{202} could

not exist in this circuit. In this condition the first spurious passband is consisted of TE_{301} and TE_{103} .

2.2. Even Modes

The formula to calculate resonant frequency of SIW cavity is given:

$$f_{i0j} = \frac{c_0}{2\sqrt{\varepsilon_r}} \sqrt{(i/a_{eff})^2 + (j/l_{eff})^2} \quad (1)$$

The relationship between SIW and equivalent RW has been illustrated. The normalized width of RW can be calculated using the following equations [6]:

$$\left\{ \begin{array}{l} \bar{a} = \xi_1 + \frac{\xi_2}{\frac{p}{\bar{d}} + \frac{(\xi_1 + \xi_2 - \xi_3)}{(\xi_3 - \xi_1)}}, \quad \xi_1 = 1.0198 + \frac{0.3465}{\frac{a}{p} - 1.0684}, \\ \xi_2 = -0.1183 - \frac{1.2729}{\frac{a}{p} - 1.2010}, \quad \xi_3 = 1.0082 - \frac{0.9163}{\frac{a}{p} + 0.2152} \end{array} \right. \quad (2)$$

The relative error of the formulae above is below 1% and the width of the equivalent RW is:

$$a_{RW} = \bar{a}a_{SIW} \quad (3)$$

Single-side shrink quantity of the transformation from post wall to equivalent EW could be written as:

$$\Delta = \frac{a_{SIW} - a_{RW}}{2} \quad (4)$$

For even mode, the gap equals electric wall and two halves of the FSIW cavity can be considered as two SIW cavities. \bar{a} and \bar{l} can be obtained by substituting a with a_{FSIW} and l_{FSIW} in (7), (8) and (9), respectively. So the effective width and length of this FSIW cavity are:

$$\left\{ \begin{array}{l} a_{eff} = 2\bar{a}a_{FSIW} \\ l_{eff} = 2\bar{l}l_{FSIW} \end{array} \right. \quad (5)$$

2.3. Odd Modes

Figure 3 shows the equivalent folded RW and scheme to calculate the capacitance in the gap region. The parameters in Figure 3(a) can be expressed by

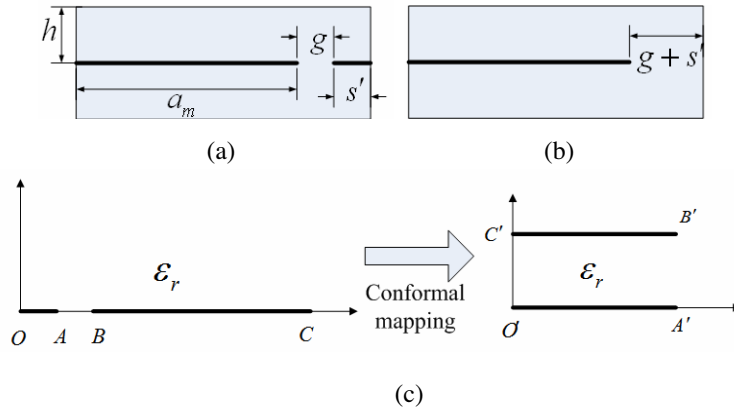


Figure 3. (a) Equivalent RW; (b) Configuration of C_1 ; (c) Conformal mapping of C_2 .

$$s' = s + d/2 - \Delta \quad (6)$$

$$a_m = a_{\text{FSIW}} - (d/2 + s + g + \Delta) \quad (7)$$

The transverse resonance condition can be written as

$$-jY_{01} \cot(k_x a_m) + j\omega(C/2) = 0 \quad (8)$$

The characteristic impedance of 2-D parallel plate waveguide is defined as

$$Z_{01} = \frac{1}{Y_{01}} = \frac{\eta h k}{k_x} \quad (9)$$

The capacitance is assumed to be small enough, use Taylor expansion to approximate the cotangent function in (13)

$$\cot(k_x a_m) \approx \frac{\pi}{2} + n\pi - k_x a_m \quad (10)$$

where n has the same meaning as the footprint of TE_{n0} .

In the condition of transverse resonance,

$$k_x = k \quad (11)$$

The cutoff wavelength of FSIW structure is approximated by

$$\lambda_c = \frac{2a_m}{(n + 1/2)} \left(1 + \frac{Ch}{2\epsilon a_m} \right) \quad (12)$$

So the equivalent width of the middle metallic plate is:

$$a_{eff} = 2a_m \left(1 + \frac{Ch}{2\epsilon a_m} \right) \quad (13)$$

Simultaneously, the equivalent length of the middle metallic plate in the cavity could be expressed as:

$$l_{eff} = 2l_m \left(1 + \frac{Ch}{2\epsilon l_m} \right) \quad (14)$$

The capacitance in Figure 3(a) can be approximately decomposed into two parts:

$$C = C_1 + C_2 \quad (15)$$

Set

$$g' = c_f g + g_0 \quad (16)$$

where $c_f = 0.73$, and $g_0 = 0.34$ mm. The reason why g should be modified is that the mutual influence between C_1 and C_2 has been taken into consideration. The metallic plate becomes longer in Figures 3(b) and (c) while the capacitive vane changes in Figure 3(c) whilst according to [16], multiple images of the gap by the top and bottom solid plates would change the capacitance of C_1 . So the overall capacitance would bring more changes on g rather than s' . In this case, the modification of g should be enough to reduce the error.

The first capacitance in (20), C_1 , which is illustrated in Figure 3(b), can be found in [16]:

$$C_1 = \frac{4\epsilon}{\pi} \ln \left[\frac{h \left(1 - \frac{g' + s'}{a_m + g' + s'} \right)}{g' + s'} \right] \quad (17)$$

Based on the assumption that the second capacitance in (20), C_2 , is introduced only by the middle metallic plate and the capacitive vane and a_m is much bigger than s' , the calculation of the capacitance can utilize the conformal mapping method. The result is shown below:

$$\begin{cases} C_2 = \frac{2\epsilon K(k_1)}{K'(k_1)} \\ k_1 = \sqrt{\frac{s'}{g' + s'}} \end{cases} \quad (18)$$

3. NUMERICAL RESULTS AND DISCUSSIONS

To verify the theoretical analysis in Section 2, the full-wave simulation is employed to compare the simulated results with the results obtained by the formulae above.

Condition 1 (C_1): $a_{\text{FSIW}} = 8.4$ mm, $l_{\text{FSIW}} = 8$ mm, $g = 0.7$ mm, $s = 0.3$ mm, $h = 1.016$ mm, and $d = 0.6$ mm.

Condition 2 (C_2): $a_{\text{FSIW}} = 8.4$ mm, $l_{\text{FSIW}} = 7.2$ mm, $g = 0.4$ mm, $s = 0.1$ mm, $h = 1.016$ mm, and $d = 0.6$ mm.

From the comparison between calculated and simulated results in Table 1, good agreement can be observed and the deviation between them is less than 1%. This demonstrates the accuracy of the proposed formulae. The resonant frequency of $TE_{(2m)0(2n)}$ is calculated based on the assumption that the gap is treated as electric wall and thus the relative error is mainly introduced by (7). In other words, the resonant frequency is independent of the capacitive vanes and the gap which plays an important role in the generation of distributed capacitance. Excellent result of TE_{202} has been obtained and the relative error, 0.08%, is much lower than the expected tolerance of the full-wave simulation. The effective length and width of the odd modes in the quarter-wavelength resonator vary with the distributed capacitance. So their resonant frequency could be controlled by the size of the vanes and the gaps.

Table 1. Calculated and simulated results for resonant frequencies.

	Calculated result (C1/C2) (GHz)	Simulated result (C1/C2)(GHz)	Relative error (C1/C2) (%)
f_{101}	8.559/8.367	8.578/8.414	0.22/0.56
f_{202}	15.641/16.683	15.628/16.657	0.08/0.16
f_{301}	18.724/17.450	18.635/17.469	0.48/0.11
f_{103}	19.543/19.889	19.496/19.866	0.24/0.12
f_{402}	24.396/25.077	24.274/25.020	0.50/0.23
f_{204}	25.061/27.618	25.105/27.555	0.18/0.23
f_{303}	25.676/25.101	25.585/25.047	0.36/0.22

4. APPLICATION

Based on the formulae deduced previously, a fourth-order bandpass filter centered at 8 GHz with the fractional bandwidth of 5% and in-

band return loss of 20 dB has been designed to validate the analysis of the FSIW cavity. The coupling of two resonators has been realized by forming an isolation post-wall and adding two capacitive vanes between them. The configuration of this proposed coupling is shown in Figure 4(a). The electric field distributions on the top metal plate have been shown in Figures 4(b) and (c).

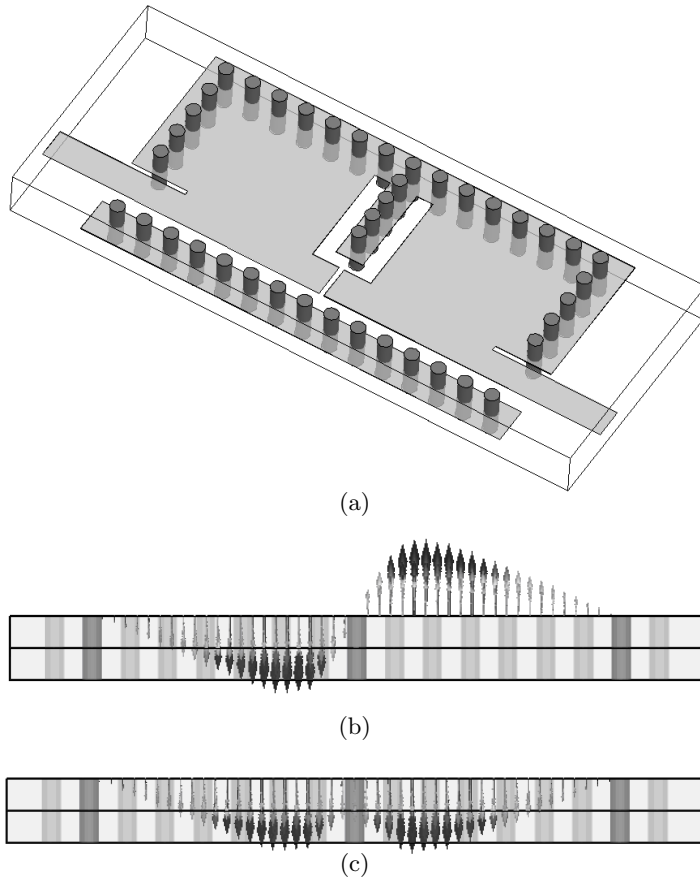


Figure 4. The proposed coupling structure. (a) Configuration; (b) Low mode; (c) High mode.

It can be concluded that these two resonators are electrically coupled since in the electric coupling structure the low mode is odd mode and the high mode is even mode [23]. The coupling strength could be easily controlled by the dimensions of the added capacitive vanes and the gap width between them. Also $50\text{-}\Omega$ stripline has been

coefficients and external quality factors [23]. The parameters shown in Figure 5(a) are $a_{\text{FSIW}} = 7.2$ mm, $l_{\text{FSIW1}} = 7.36$ mm, $l_{\text{FSIW2}} = 7.43$ mm, $g = 0.7$ mm, $s = 0.3$ mm, $d = 0.6$ mm, $d_{io} = 1.32$ mm, $a_{12} = 0.92$ mm, $a_{23} = 0.92$ mm, $a_{14} = 0.6$ mm, $b_{12} = 0.2$ mm, $b_{23} = 0.2$ mm, $b_{14} = 0.4$ mm, $l_c = 1.25$ mm and $W_{\text{strip}} = 1.3$ mm.

A prototype of the bandpass filter is fabricated by multilayer standard PCB process on the substrate of Taconic TSM-30 with the height of 1.016 mm and 0.888 mm for the upper and lower layer respectively and the prepreg of Taconic TPN-30 with the height of 0.128 mm, which is shown in Figure 5(c). The relative dielectric constants of these two materials are both 3.0 and the loss tangent of TSM-30 is 0.0015. The total size of this folded substrate integrated waveguide bandpass filter is 14.8 mm \times 14.4 mm \times 2.032 mm itself. Obviously the proposed design is very compact.

The fabricated filter is measured with a vector network analyzer HP8722ES. For the measurement convenience, the transition between the stripline and the grounded coplanar waveguide (GCPW) has been used. The measured performances of the fourth-order filter are illustrated in Figure 6, as well as the simulated results. The measured central frequency of the fundamental band is 7.8 GHz and FBW is 6%. The first spurious passband appears at approximately 16.8 GHz and S_{21} is over 20 dB from 9 GHz to 16 GHz, implying wide out-of-band rejection.

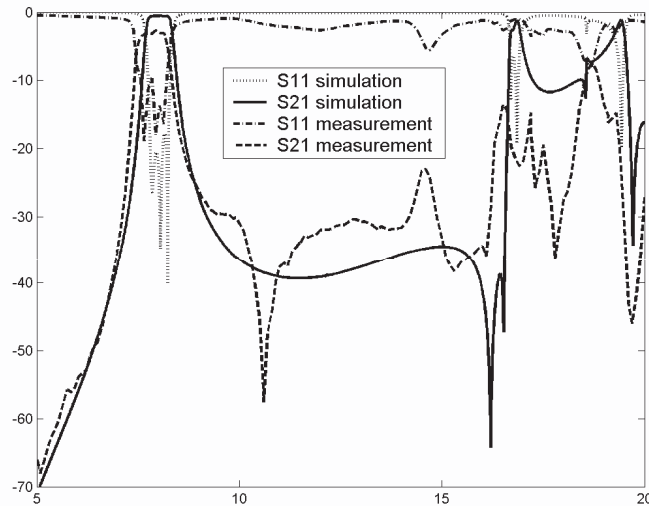


Figure 6. Simulated and measured results of FSIW BPF.

The center frequency deviation of experiment and the simulation is about 2.5%, probably owing to low processing precision. The measured insertion loss is approximately 2.62 dB and the return loss is below 10 dB. There are several reasons for the deviations of experiment parameters from simulation parameters. Firstly, the conductor loss of this filter has not yet been brought into consideration in the full wave simulation. Secondly, the I/O terminal lines are composed of SMA connector, GCPW and stripline when measuring. The discontinuity between SMA connectors and GCPW and the transition between GCPW and stripline should affect the original frequency response, and thus brings more reflection and conductor loss. Thirdly, the loss tangent of TPN-30 prepreg is bigger than that of TSM-30, which implies that more dielectric loss is introduced. Moreover the inaccuracy in PCB manufacturing process may also influence the overall frequency response.

5. CONCLUSIONS

This paper provides formulae of the cavity and verified by full-wave simulation. An example of filter operating at 8 GHz is presented, together with s -parameter curves to verify the formulae provided. The proposed filter has the advantage of wide out-of-band rejection and compact size, and it can be applied to low-cost microwave and millimeter wave integrated circuits and thus the formulae deduced can enhance the efficiency of the filter design.

ACKNOWLEDGMENT

This work was supported in part by CMRFT, Shanghai Jiaotong University and also in part by Taconic Advanced Material Co., Ltd. The authors wish to express their gratitude to Dr. Qi-Fu Wei of CMRFT, Shanghai Jiaotong University, for his helpful comments and discussions.

REFERENCES

1. Hirokawa, J. and M. Ando, "Single-layer feed waveguide consisting of posts for plane TEM wave excitation in parallel plates," *IEEE Trans. Antennas and Propag.*, Vol. 46, No. 5, 625–630, May 1998.
2. Deslandes, D. and K. Wu, "Integrated microstrip and rectangular waveguide in planar form," *IEEE Microwave and Wireless Components Letters*, Vol. 11, No. 2, 68–70, Feb. 2001.

3. Cassivi, Y., L. Perregriani, P. Arcioni, M. Bressan, K. Wu, and G. Conciauro, "Dispersion characteristics of substrate integrated rectangular waveguide," *IEEE Microwave and Wireless Components Letters*, Vol. 12, No. 9, 333–335, Sept. 2002.
4. Deslandes, D. and K. Wu, "Accurate modeling, wave mechanisms, and design considerations of a substrate integrated waveguide," *IEEE Trans. Microw. Theory Tech.*, Vol. 54, No. 6, 2516–2526, Jun. 2006.
5. Talebi, N. and M. Shahabadi, "Application of generalized multipole technique to the analysis of discontinuities in substrate integrated waveguides," *Progress In Electromagnetics Research*, PIER 69, 227–235, 2007.
6. Yan, L., W. Hong, G. Hua, J. Chen, K. Wu, and T. Cui, "Simulation and experiment on SIW slot array antennas," *IEEE Microwave and Wireless Components Letters*, Vol. 14, No. 9, 446–448, Sept. 2004.
7. Che, W., E. K. N. Yung, K. Wu, and X. Nie, "Design investigation on millimeter-wave ferrite phase shifter in substrate integrated waveguide," *Progress In Electromagnetics Research*, PIER 45, 263–275, 2007.
8. Hao, Z., W. Hong, X. Chen, J. Chen, K. Wu, and T. Cui, "Multilayered substrate integrated waveguide (MSIW) elliptic filter," *IEEE Microwave and Wireless Components Letters*, Vol. 15, No. 2, 95–97, Feb. 2005.
9. D’Orazio, W. and K. Wu, "Substrate-integrated-waveguide circulators suitable for millimeter-wave integration," *IEEE Trans. Microw. Theory Tech.*, Vol. 54, No. 10, 3675–3680, Oct. 2006.
10. Djerafi, T. and K. Wu, "Super-compact substrate integrated waveguide cruciform directional coupler," *IEEE Microwave and Wireless Components Letters*, Vol. 17, No. 11, 757–759, Nov. 2007.
11. Zhang, Z.-Y. and K. Wu, "A broadband substrate integrated waveguide (SIW) planar balun," *IEEE Microwave and Wireless Components Letters*, Vol. 17, No. 12, 843–845, Dec. 2007.
12. Zhang, X.-C., Z.-Y. Yu, and J. Xu, "Novel band-pass substrate integrated waveguide (SIW) filter based on complementary split ring resonators (CSR), " *Progress In Electromagnetics Research*, PIER 72, 39–46, 2007.
13. Han, S., X. Wang, Y. Fan, Z. Yang, and Z. He, "The generalized Chebyshev substrate integrated waveguide diplexer," *Progress In Electromagnetics Research*, PIER 73, 29–38, 2007.
14. Chen, G. L., T. L. Owens, and J. H. Whealton, "Theoretical study

- of the folded waveguide,” *IEEE Trans. Plasma Sci.*, Vol. 16, No. 2, 305–308, Apr. 1998.
15. Grigoropoulos, N., B. S. Izquierdo, and P. R. Young, “Substrate integrated folded waveguides (SIFW) and filters,” *IEEE Microwave and Wireless Components Letters*, Vol. 15, No. 12, 829–831, Dec. 2005.
 16. Che, W., L. Geng, K. Deng, and Y. L. Chow, “Analysis and experiments of compact folded substrate-integrated waveguide,” *IEEE Trans. Microw. Theory Tech.*, Vol. 56, No. 1, 88–93, Jan. 2008.
 17. Izquierdo, B. S., P. R. Young, N. Grigoropoulos, J. C. Batchelor, and R. J. Langley, “Substrate-integrated folded waveguide slot antenna,” *Proc. IEEE Small Antennas Novel Meta Mater.*, 307–309, Sept. 2005.
 18. Geng, L., W. Che, and K. Deng, “Wideband bandpass filter of folded substrate-integrated waveguide integrating with stripline compact resonant cell,” *Microw. Opt. Technol. Lett.*, Vol. 50, No. 2, 390–393, Feb. 2008.
 19. Lei, W., W. Che, K. Deng, and S. Dong, “Narrow-slot bandpass filter based on folded substrate integrated waveguide with wide out-of-band rejection,” *Microw. Opt. Technol. Lett.*, Vol. 50, No. 5, 1155–1159, May 2008.
 20. Hong, J.-S., “Compact folded-waveguide resonators,” *IEEE MTT-S Digest*, 213–216, 2004.
 21. Alotaibi, S. K. and J.-S. Hong, “Novel substrate integrated waveguide filter,” *Microw. Opt. Technol. Lett.*, Vol. 50, No. 4, 1111–1114, Apr. 2008.
 22. Lin, H., “Novel folded resonators and filters,” *IEEE MTT-S Digest*, 1277–1280, 2007.
 23. Hong, J.-S. and M. J. Lancaster, *Microstrip Filter for RF/Microwave Applications*, Wiley-Interscience, New York, 2000.
 24. Amari, S., “Synthesis of cross-coupled resonator filters using an analytical gradient-based optimization technique,” *IEEE Trans. Microw. Theory Tech.*, Vol. 48, No. 9, 1559–1564, Sep. 2000.